

Efficient functionalization of alginate biomaterials

Marianne Ø. Dalheim¹, Julie Vanacker², Maryam A. Najmi¹, Finn L. Aachmann¹, Berit L. Strand¹ and Bjørn E. Christensen^{1*}

¹ *NOBIPOL, Department of Biotechnology, Norwegian University of Science and Technology (NTNU), Trondheim N-7491, Norway*

² *Advanced Drug Delivery and Biomaterials, Louvain Drug Research Institute, Université catholique de Louvain (UCL), Brussels B-1200, Belgium*

*Corresponding author

Address for correspondence:

Bjørn E. Christensen

NTNU, Department of Biotechnology

Sem Sælands veg 6/8

N-7491 Trondheim

Norway

E-mail: bjorn.e.christensen@ntnu.no

Phone: +47 73 59 33 27

Fax: +47 73 59 12 83

Abstract

Peptide coupled alginates obtained by chemical functionalization of alginates are commonly used as scaffold materials for cells in regenerative medicine and tissue engineering. We here present an alternative to the commonly used carbodiimide chemistry, using partial periodate oxidation followed by reductive amination. High and precise degrees of substitution were obtained with high reproducibility, and without formation of by-products. A protocol was established using L-Tyrosine methyl ester as a model compound and the non-toxic pic-BH_3 as the reducing agent. DOSY was used to indirectly verify covalent binding and the structure of the product was further elucidated using NMR spectroscopy. The coupling efficiency was to some extent dependent on alginate composition, being most efficient on mannuronan. Three different bioactive peptide sequences (GRGDYP, GRGDSP and KHIFSDDSSE) were coupled to 8 % periodate oxidized alginate resulting in degrees of substitution between 3.9 and 6.9 %. Cell adhesion studies of mouse myoblasts (C2C12) and human dental stem cells (RP89) to gels containing various amounts of GRGDSP coupled alginate demonstrated the bioactivity of the material where RP89 cells needed higher peptide concentrations to adhere.

Keywords

Alginate, periodate oxidation, reductive amination, cell adhesion, RGD peptide, tissue engineering

Introduction

The use of biomaterials has expanded over the last years including the use of hydrogels of natural polymers such as alginates, agarose, collagen, gelatin, fibrin and hyaluronic acid in regenerative medicine and tissue engineering. The biomaterial may give structural support and provide various biological signals to the cells in the matrix [1]. In tissue engineering the aim is to make functional tissues and organs for transplantation and the general idea is that cells should be seeded in or attracted to a material mimicking the extracellular matrix (ECM) to allow stable and functional tissue formation. The ECM is, however, a complex material providing mechanical support (scaffold), growth factors, nutrients and other important factors for development of cell phenotype as well as tissue formation [2]. Alginates have been used as the scaffold material for mammalian cells in both 2D and 3D cultures in many studies and this has been thoroughly reviewed elsewhere [3, 4]. Alginates are well suited for these applications due to their ability to form soft hydrogels at physiological conditions with pores large enough for nutrients and growth factors to pass freely while cells are entrapped within the polymer network. Among their beneficial features is also their low toxicity and high biocompatibility [4, 5].

Alginates are a group of unbranched polysaccharides composed of 1,4-linked β -D-mannuronic acid (M) and α -L-guluronic acid (G) produced by brown seaweeds and some bacteria. It is synthesized as

homopolymeric mannuronan, and G residues are introduced post polymerization by enzymatic epimerization at C5. Alginates have no regular structure but have stretches of continuous M or G residues and sequences of alternating M and G, referred to as M-blocks, G-blocks and MG-blocks respectively [3]. Alginate hydrogels are formed by ionic crosslinking of G-blocks (with some contribution from the MG-blocks [6]) by certain divalent cations (e.g. Ca^{2+} , Ba^{2+} and Sr^{2+}). The relative amounts of M and G and the length of the different block structures therefore affect the gel forming ability and the mechanical properties of the gels [7-9]. Alginates isolated from different sources vary in both composition and block structure. Today, it is also possible to prepare alginates with tailored properties *in vitro* using mannuronan from an epimerase deficient *Pseudomonas fluorescens* mutant [10] as substrate, and a set of epimerases with different specificities and processivities, isolated from alginate producing bacteria [7, 8, 11].

Alginate itself does not contain any sites for cell attachment or other specific receptor interactions, although some alginates have been shown to influence keratinocyte morphology and gene expression in a structure- or calcium-dependent manner [12]. To induce cell interaction, bioactive peptide sequences that are known to bind to receptors on the cell surfaces can be covalently linked to the alginate [13-15]. These bioactive peptides will mimic both the adhesive properties of ECM proteins containing these sequences and the stimulation of cellular responses such as differentiation and proliferation. A variety of such peptides has been identified and used in cell attachment studies and in particular the tripeptide sequence RGD (Arginine-Glycine-Aspartic acid) because of its abundance in adhesion proteins (e.g. fibronectin, laminin, fibrinogen, vitronectin etc.) and its ability to bind to a wide variety of integrins [16]. Another example is KHIFSDDSSSE which is the rat homologue to the shortest peptide sequence mimicking the homophilic binding region in N-CAMs [17]. Rat cortical astrocytes have been shown to adhere to substrates modified with this peptide [18].

Alginate modifications with bioactive peptides are traditionally accomplished by carbodiimide chemistry and have shown to give around 0.1 – 1.0 % mol peptide per mol uronate monomer [14, 19, 20]. Although peptide densities in this concentration range do induce attachment of myoblasts [14, 20], olfactory ensheathing cells [20], mesenchymal stem cells [13] and endothelial cells [21], increasing densities of peptides influence the impact on cells related to both attachment and differentiation as shown by Rowley and Mooney for C2C12 myoblasts on RGD-alginate [14]. Different peptide concentrations have also been shown to impact both the number of attached cells and cellular differentiation for neuroblastomas on YIGSR peptide-alginate [22]. Increasing the degree of peptide substitution is relevant for the use of peptide-alginate mixed in with non-substituted alginates in the bulk phase to form bioactive hydrogels and as coating materials in e.g. alginate foams [23]. Carbodiimide chemistry is also associated with the formation of urea derivatives and N-acylurea bound to the alginate [20] contributing to a destruction of gelling properties without the addition of bioactivity.

Periodate oxidation of polysaccharides has traditionally been used as a method for structure determination of carbohydrates. More recent research has, however, focused on the new properties that are introduced in oxidized polysaccharides. Periodate ions (IO_4^-) will react with polysaccharides in a specific manner oxidizing vicinal diols and other closely related structures [24, 25]. In the case of alginates, periodate oxidation results in stoichiometric cleavage of the C2-C3 bond and introduction of an aldehyde at both C2 and C3 as illustrated in Figure 1. The ring opening has a substantial effect on the overall chain extension and gives a more flexible polymer [26-28]. In addition the oxidized alginates are more degradable which is proposed as favorable in tissue engineering [29].

Reductive amination is a two-step reaction between a carbonyl and an amine, with formation of a Schiff base as the first step and subsequently reduction to a stable secondary amine (Figure 1). The traditional reducing agent has been sodium cyanoborohydride (NaBH_3CN) but alternative reducing agents have been sought to avoid the possible formation of poisonous hydrogen cyanide during the reaction when using NaBH_3CN . Sato and coworkers [30] showed that 2-methylpyridine borane complex (pic-BH_3) can be an equally efficient and non-toxic alternative to NaBH_3CN . Pic-BH_3 has been utilized in studies of end labelling of glycans [31, 32]. Recently, an example of coupling of amino acids to oxidized cellulose using reductive amination with pic-BH_3 has been reported [33].

Here, we report an alternative method for high efficiency coupling of bioactive peptides to alginates using periodate oxidation followed by reductive amination with the non-toxic pic-BH_3 as the reducing agent. The main focus has been on the optimization of the process and chemical characterization. Alginates with covalently attached GRGDSP was used to demonstrate the activity of the material and the effect of high peptide densities on the attachment of mouse skeletal myoblasts (C2C12) and human dental stem cells (RP89 cells) to peptide-alginate hydrogels.

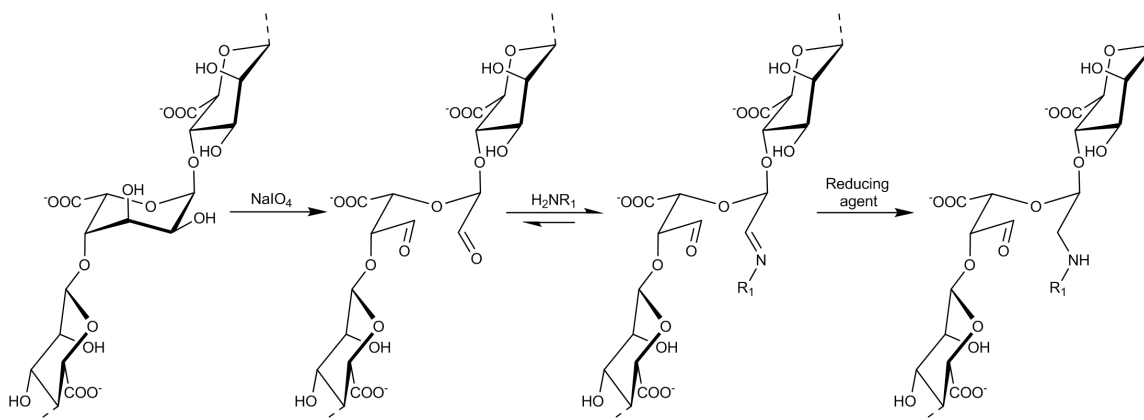


Figure 1: The coupling strategy. Alginate, here represented by an MGM fragment is first partially oxidized (typically $D_{\text{ox}} = 8\%$). In the second step the oxidized polymer is reacted with a primary amine forming a Schiff base which is further reduced to a stable amine.

Materials and methods

Materials and chemicals

Alginates from *Laminaria hyperborea* stipe and leaf were obtained from FMC Biopolymer, Drammen, Norway. Mannuronan was isolated from an epimerase-negative mutant of *Pseudomonas fluorescens* [10]. A bacterial alginate with 6 % G residues was isolated from *Pseudomonas aeruginosa* [34] and an alginate with 85 % G was obtained by epimerizing mannuronan with the epimerases AlgE4 and AlgE6 as previously described [7]. The composition (determined by ¹H-NMR) and molecular weight (determined by SEC-MALS) of the different alginates are given in Table 1.

Table 1: Composition and molecular weight (M_w) of the alginates in this study.

Alginate	F _G	F _M	F _{GG}	F _{MG} F _{GM}	F _{MM}	F _{MGG} F _{GGM}	F _{MGM}	F _{GGG}	N _{G>1}	M_w (kDa)
Mannuronan	0.00	1.00	0.00	0.00	0.00	0.00	0.00	0.00	0	900
Bacterial high-M alginate	0.06	0.93	0.00	0.06	0.87	0.00	0.06	0.00	0	170
Leaf alginate	0.46	0.54	0.29	0.17	0.37	0.05	0.15	0.24	7	220
Stipe alginate	0.65	0.35	0.53	0.12	0.23	0.05	0.10	0.48	11	110
In vitro epimerized alginate	0.85	0.15	0.77	0.08	0.07	0.03	0.06	0.74	24	210

The peptides, GRGDYP, GRGDSP and KHIFSDDSSE, were purchased from CASLO ApS, Denmark. All other chemicals were obtained from commercial sources and were of analytical grade.

Periodate oxidation

The alginates were dissolved in MQ-water (deionized water purified with the MilliQ system from Millipore, Bedford, MA, USA) to a final concentration of 4.4 mg/ml - 8.8 mg/ml depending on the viscosity of the solution. 10 % (v/v) of propanol was added as a free radical scavenger and the solution was degassed using nitrogen gas and cooled down to 4°C. Sodium (meta)periodate (NaIO₄, Merck) was prepared as a 0.25 M solution in MQ-water, degassed (nitrogen) and added stoichiometrically to the alginate solution according to the desired degree of oxidation ($D_{ox} = P_0$ (periodate/monomer molar ratio) x 100 %). All handling was carried out in subdued light. The reaction was carried out at 4°C for 48-72 hours and the samples were thereafter dialyzed against MQ-water at 4°C until the conductivity was below 2 μS and freeze-dried.

Reductive amination

The influence of different reaction parameters on the degree of coupling was tested varying one while holding the others constant. In the following procedure the concentration/condition in parenthesis is the final concentration/condition in the optimized protocol.

Periodate oxidized alginate (POA) or mannuronan (POM) was dissolved in MQ-water to a stock concentration of 6 mg/ml. Methanol (MeOH) was added to its final concentration (12 % (v/v)) before addition of 0.25 M L-Tyrosine methyl ester (MeOTyr, Sigma-Aldrich) in MeOH (2.42 mM) and 0.25 M pic-BH₃ (Sigma-Aldrich) in MeOH (24.24 mM). The pH was adjusted to the desired pH (pH 5.8), using 1M Acetate buffer pH 5.0, and MQ-water was added to achieve a final alginate concentration of 3 mg/ml (1.21 mM oxidized residues if D_{ox} = 8 %). The samples were incubated on a shaker for 6, 24 or 48 hours (48 h) at the desired temperature (room temperature). All samples were dialyzed against two shifts of 0.05 M NaCl and then MQ-water until the conductivity was less than 2 μS and finally freeze-dried.

The optimized protocol was used in coupling of peptides. The peptides were added as 0.05 M GRGDSP, GRGDYP or KHIFSDDSSSE in water to a final concentration of 2.42 mM.

NMR sample preparation

All alginate samples were subjected to mild acid hydrolysis as previously described [35] to reduce the viscosity prior to NMR analysis. 6-8 mg of the samples were then dissolved in 600 μl D₂O (99.9 %) and added 5 μl 3-(Trimethylsilyl)propionic 2,2,3,3-d₄ acid (Sigma Aldrich) as an internal standard. Samples of POA coupled to MeOTyr (POA-MeOTyr) were in addition added 15 μl Triethylenetetraamine-hexaacetic acid (Sigma Aldrich) as a chelating agent for residual divalent ions.

NMR acquisition and analysis

All homo- and heteronuclear NMR experiments were carried out on a BRUKER Avance DPX 300 MHz, 400 MHz or 600 MHz spectrometer (Bruker BioSpin AG, Fällanden, Switzerland) equipped with a 5 mm QNP, 5 mm z-gradient DUL (C/H) and 5-mm cryogenic CP-TCI z-gradient probe, respectively. The degree of substitution (DS = moles of substituents per mole of alginate monomer) was determined from a 1D ¹H spectrum recorded at 90°C on the 300 or 400 MHz spectrometer and calculated as the molar percentage (% of the alginate residues having a substituent).

For chemical shift assignment, the following spectra were recorded: 1D ¹H, 2D double quantum filter correlated spectroscopy (DQF-COSY), 2D in-phase correlation spectroscopy (IP-COSY) [36], 2D total correlation spectroscopy (TOCSY) with 70 ms of mixing time, 2D ¹³C heteronuclear single quantum coherence (HSQC) with multiplicity editing, 2D ¹³C HSQC-[¹H,¹H]TOCSY with 70 ms of mixing time on protons, and 2D heteronuclear multibond correlation (HMBC) with BRID filter to

suppress first order correlation. These spectra were all recorded at 25°C on the 600 MHz spectrometer.

Diffusion-Ordered Spectroscopy (DOSY) was used to measure the diffusion of the coupled products. A 2D DOSY was setup using a Bruker BioSpin stimulated echo pulse sequence with bipolar gradients (STEBPGP). Gradient pulses of 1.5 ms duration (δ) and 32 different strengths varying linearly from 0.03 to 0.57 T·m⁻¹ was applied and the diffusion delay (Δ) was set to 500 ms. The DOSY spectrum was recorded at 25°C on the 600 MHz spectrometer.

The spectra were recorded using TopSpin 1.3 or 2.1 software (Bruker BioSpin) and processed and analyzed with TopSpin 3.0 software (Bruker BioSpin).

Low molecular weight POM-MeOTyr for structural analysis by NMR

A sample with high degree of MeOTyr coupled onto mannuronan was prepared to ease the structural analysis. Mannuronan was subjected to mild acid hydrolysis according to the NMR sample preparation protocol. The degraded sample was oxidized using an amount of periodate ions corresponding to a $D_{ox} = 40\%$ and then coupled to MeOTyr using the optimized protocol.

UV spectroscopy

UV spectrophotometry was used to analyze DS. Samples of stipe POA-MeOTyr and POM-MeOTyr were dissolved in MQ water (0.1 %, w/v) and a UV absorbance spectra (230-330 nm) was acquired for three parallels each in a 96 wells UV transparent microplate (Costar), using a multimode reader (Infinite 200 PRO, TECAN). Stipe POA and POM in MQ-water (0.1 wt. %) was used as blanks. All samples were dried in a desiccator overnight prior to analysis. The background absorbance was corrected for using the absorbance ratio A_{274}/A_{310} of the blank samples and A_{310} of the samples to find the absorbance originating from the substituent MeOTyr at 274 nm. Absorbance was converted to concentration using a calibration curve for absorbance at 274 nm as a function of the concentration of MeOTyr in MQ-water and the DS was calculated as the molar percentage (% of the alginate residues having a substituent).

SEC-MALS

The molecular weight of MeOTyr coupled samples was analyzed by Size Exclusion Chromatography with Multi Angle Light Scattering (SEC-MALS). Samples and standards dissolved in the mobile phase (0.05M Na₂SO₄ with 0.01M EDTA, pH 6.0) were injected on an HPLC system consisting of a mobile phase reservoir, an on-line degasser, an HPLA isocratic pump, an autoinjector, a precolumn and two serially connected columns (TSK 5000 PWXL, and TSK 4000 PWXL). The column outlet was connected to two serially connected detectors, a Dawn DSP multiangle laser light scattering photometer (Wyatt, USA) ($\lambda_0 = 0.633$ nm) followed by an Optilab DSP differential refractometer (P-

10 cell) (Wyatt, USA). The analysis was carried out at ambient temperature with a flow rate of 0.5 ml/min. Injection volume and sample concentration was adjusted to obtain an optimal light scattering signal without influencing the RI profile (overloading). All samples were filtered (pore size 0.8 μm) prior to injection. Astra software v. 6.1 (Wyatt, USA) was used to collect and process the data obtained from the light scattering and the differential refractometer, using a refractive index increment (at constant chemical potential), $(dn/dc)_\mu$ of 0.150 ml/g [28] for alginate samples.

Cell culture

Mouse skeletal myoblast cell-type C2C12 was purchased from ATCC (CRL-1772) and cells were cultured in DMEM (Sigma-Aldrich) supplemented with 10 % FCS, 4 mM glutamine and 20 $\mu\text{g/ml}$ gentamicin at 37°C and 5 % CO_2 . The cells were kept in sub-confluent culture until the start of the experiment in order to avoid differentiation.

Human dental stem cells (RP89 cells) were isolated from the apical papilla of immature permanent teeth, purified and fully characterized as previously described by Ruparel et al. [37]. Cells were grown at 37°C and 5 % CO_2 in Minimum Essential Medium (Sigma–Aldrich) supplemented with 10 % bovine serum, 1 % of L-glutamine and 1 % of penicillin and streptomycin. The cells were kept in sub-confluent culture until the start of the experiment in order to avoid differentiation.

Preparation of calcium alginate hydrogels

Stipe alginate alone, or combined with 2.5 %, 6.25 %, 12.5 % or 25 % (w/w) of leaf POA coupled to GRGDSP (leaf POA-GRGDSP) were dissolved at a concentration of 2 % (w/v) in 3 ml of MQ water, corresponding to final peptide concentrations of 0.1 %, 0.25 %, 0.5 % and 1.0 % mol peptide per mol uronic acids respectively. As controls, the same stipe alginate combined with 2.5 %, 6.25 %, 12.5 % or 25 % (w/w) of leaf POA was dissolved similarly. The alginate solutions were filtered on 0.22 μm sterile filters. 500 μl of an autoclaved calcium carbonate solution (CaCO_3 , Eskal 500, KSL Staubtechnik GMBH) was added to 1.5 ml of each alginate solution to obtain a final concentration of 15 mM. A solution of D-(+)-gluconic acid δ -lactone (GDL, Sigma-Aldrich) was freshly prepared with MQ water and sterile filtered. 1 ml was then added to the different alginate- CaCO_3 solutions to a final concentration of 30 mM. Each alginate (1 % w/v) - CaCO_3 (15 mM) - GDL (30 mM) solution were distributed in a 24 wells plate (Costar) (triplicate, 400 $\mu\text{l/well}$) and the solutions were allowed to gel for 24 hours at 37°C.

Cell culture on alginate gels

19000 cells/well (RP89 or C2C12) were added carefully on top of the different alginate hydrogels with 0.5 ml of culture media per well and were incubated at 37°C and 5 % CO_2 for 48 hours. Images were captured with an Axioscope II, Carl Zeiss

Results

Determination of degree of substitution by NMR spectroscopy

All samples were analyzed by NMR spectroscopy. Typical ^1H -spectra for MeOTyr-coupled periodate oxidized mannuronan (POM-MeOTyr) and a MeOTyr-coupled periodate oxidized stipe alginate (stipe POA-MeOTyr) are shown in Figure 2A and 2B, respectively. The anomeric protons in alginates will have chemical shifts in the region 4.3-5.3 ppm [38, 39]. MeOTyr has four aromatic protons (H_δ and H_ϵ) that will give signals at higher chemical shifts (6.8 – 7.3 ppm) compared to alginate. The degree of substitution (DS), given as the ratio of substituted alginate residues to the total number of alginate residues in percent (mol/mol), can be estimated from the intensity of the signals from the aromatic protons in MeOTyr compared to the anomeric protons in the alginate chain. DS can be estimated correspondingly for peptide sequences containing aromatic amino acids, taking into account their number of aromatic protons.

Optimization of coupling protocol: POA-MeOTyr

The optimal conditions for coupling of primary amines to periodate oxidized alginates, using reductive amination with pic-BH₃ as the reducing agent, were found through a series of experiments. This included testing the influence of concentration of substituent, concentration of reducing agent, temperature and pH using the same batch of stipe POA ($D_{\text{ox}} = 8\%$) in all the optimization experiments. A D_{ox} of 8 % was chosen to ensure well detectable signals in NMR at both high and low coupling efficiencies. MeOTyr was used as a model compound to mimic coupling of peptides, where the negative charge of the carboxyl group is masked by a methyl ester group when compared to tyrosine. Overall, we were able to obtain high DS, in the range 2-6 %, for all combinations of reaction parameters (see Figure 2 C-F). Both the rate of reaction and the plateau DS values at 48 h increased with increasing concentration of substituent ([MeOTyr]) (Figure 2C). The DS could be substantially increased by increasing the concentration of the reducing agent ([pic-BH₃]). At the lowest [MeOTyr] a tenfold increase in [pic-BH₃], corresponding to an increase in the ratio of oxidized residues to pic-BH₃ from 1:2 to 1:20, increased the DS from 3.5 % to 5.7 % (Figure 2F). This was the highest DS obtained for this batch of stipe POA implying that the effect of increasing [pic-BH₃] was larger than the effect of increasing [MeOTyr].

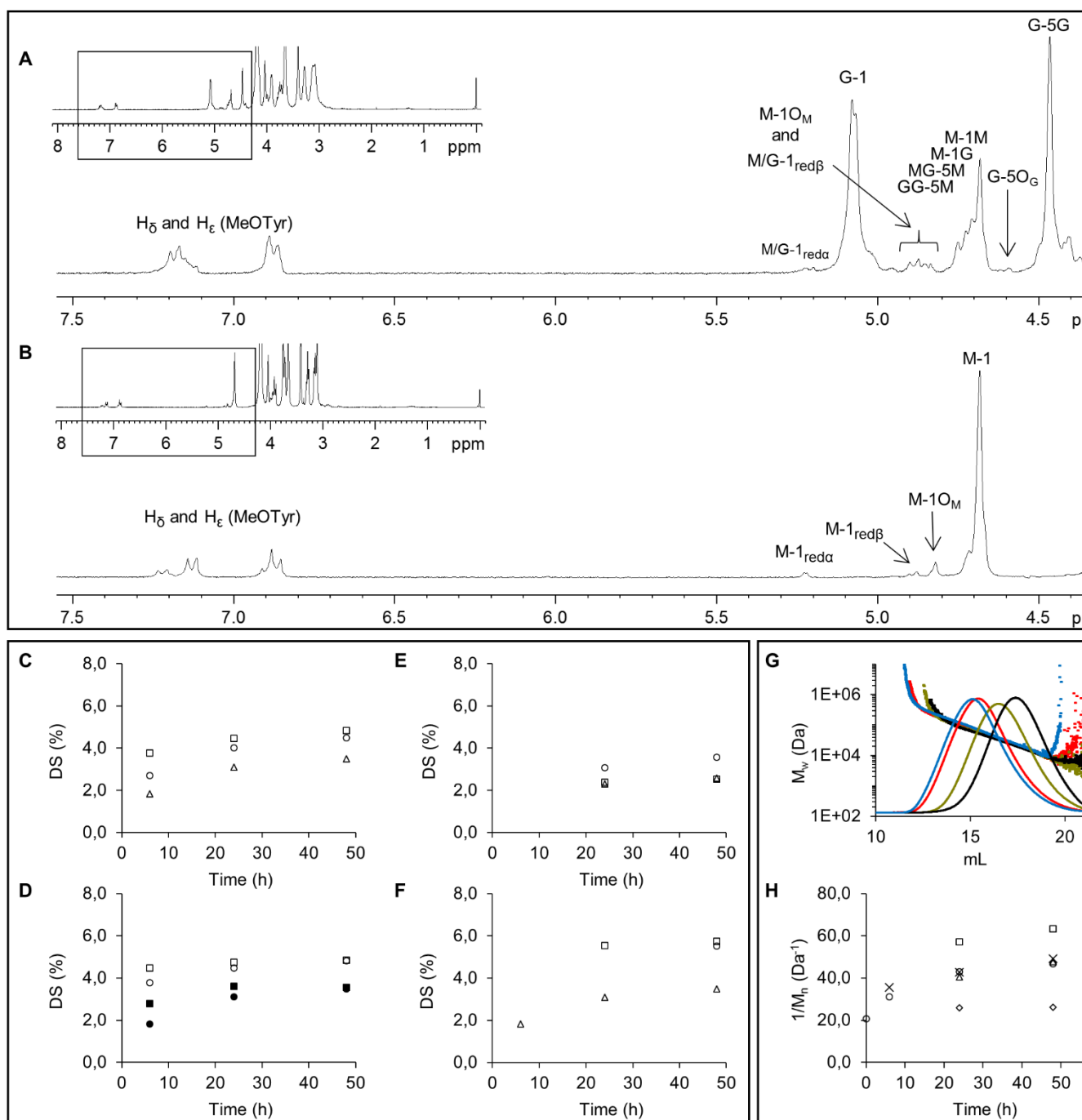


Figure 2: $^1\text{H-NMR}$ spectra (300 MHz, 90°C), of A: *L. hyperborea* stipe POA-MeOTyr and B: POM-MeOTyr in 99.9 % D_2O . The spectra are annotated according to Grasdalen et al [38, 39] and Kristiansen et al [40]. C-F: DS (mol/mol %), as a function of reaction time after coupling of MeOTyr to *L. hyperborea* stipe POA (1.21mM oxidized residues, Dox = 8 %) varying C: Concentration of MeOTyr, Δ : 2.42 mM, \circ : 7.27 mM and \square : 24.24 mM at constant pic-BH3 concentration (2.42 mM), pH 5.8 and room temperature, D: Temperature, \circ : Room temperature and \square : 37°C using 2.42 mM MeOTyr (filled symbols) and 24.24 mM MeOTyr (open symbols) at constant pic-BH3 concentration (2.42 mM) and pH 5.8, E: pH, Δ : pH 4.5 \circ : pH 5.8 and \square : pH 7.5 using 2.42 mM MeOTyr and 2.42 mM pic-BH3 at room temperature and F: Concentration of pic-BH3, Δ : 2.42 mM, \circ : 12.10 mM and \square : 24.24 mM at constant concentration of MeOTyr (2.42 mM), pH 5.8 and room temperature. G: SEC-MALS data for some selected samples. Concentration profile (solid lines) and slice molecular weights (dotted lines) for (left to right) *L. hyperborea* stipe POA (Dox = 8 %) (blue), and stipe POA-MeOTyr after reductive amination (48 h) at pH 4.5 (red), pH 5.8 (green) and pH 7.5 (black). H: $1/M_n$ (Da^{-1}) vs time of reaction at \diamond : pH 4.5, \circ : pH 5.8 and \square : pH 7.5 using 2.42 mM MeOTyr and 2.42 mM pic-BH3 at room

temperature, Δ : 2.42 mM MeOTyr and 24.24 mM pic-BH₃ at pH 5.8 and room temperature, and x : 37°C using 2.42 mM MeOTyr and 2.42 mM pic-BH₃ at pH 5.8.

Increasing the temperature from room temperature to 37°C had a small and positive effect on the rate of substitution as illustrated for reactions using concentrations corresponding to 1:2:2 and 1:20:2 ratios of oxidized residues to MeOTyr to pic-BH₃, respectively (Figure 2D). However, the plateau DS values at 48 h did not increase. Also, highest DS was obtained for pH 5.8 compared to pH 4.5 and 7.5 (Figure 2E).

All in all this resulted in an optimized protocol using a 1:2:20 molar ratio of oxidized residues:substituent:pic-BH₃, at pH 5.8 and room temperature, reacted for 48 h.

The molecular weight distributions of all samples from the optimization experiments were determined using SEC-MALS. Some examples of chromatograms and slice molecular weights are shown in Figure 2G. The oxidation itself was accompanied by some degradation and for the stipe alginate the number molecular weight average (M_n) was reduced from 56.5 kDa to 48.5 kDa during the oxidation ($D_{ox} = 8\%$) (data not shown). However, the degradation was somewhat more extensive during the reductive amination (Figure 2H). Changing the concentrations of MeOTyr and pic-BH₃ as well as increasing the reaction temperature from room temperature to 37°C had only a marginally effect. However, pH was affecting the molecular weight with increasing degradation at higher pH.

Verification of covalent coupling

Diffusion-Ordered Spectroscopy (DOSY) was used to indirectly verify that POM and MeOTyr were covalently linked after the coupling reaction. The signals for both MeOTyr and POM appeared with the same diffusion coefficient (Figure 3A, right) indicating that the coupling was successful. Similar results were also obtained for POA-MeOTyr samples, and none of the tested samples showed traces of non-reacted MeOTyr. As a negative control a 2D DOSY spectrum was recorded on a mixture of non-coupled POM and MeOTyr showing two distinct diffusion coefficient for the molecules (Figure 3A, left). The DOSY experiment is an indirect qualitative method to show that the coupling has been successful. A structural elucidation by NMR was therefore performed to obtain direct proof of the structure for the coupled product. To ease this analysis the spectra were recorded on a highly MeOTyr substituted sample prepared from low molecular weight POM (theoretical DS = 40%). The signals were assigned by starting at the anomeric signal for alginate and at the aromatic signals for MeOTyr and then following the proton-proton connectivity using TOCSY, DQF-COSY/IP-COSY, and ¹³C HSQC-[¹H, ¹H] TOCSY. The connectivity between the aromatic part and H β for MeOTyr was obtained from the HMBC spectrum allowing complete assignment of MeOTyr. Furthermore, the HMBC spectrum was also used to follow the connectivity between MeOTyr H α and carbon 2 or 3 in the alginate (see Figure 3B). These experiments showed clearly that MeOTyr is covalently bound to C2 or C3 of the oxidized sugar residue. Furthermore, two signals indicating formation of two

additional methylene CH₂ groups is observed in the ¹³C HSQC spectrum. This might be a product from the reduction with pic-BH₃, where the non-reacted aldehyde group on C2 or C3 has been reduced to a primary alcohol group. Altogether, the NMR results suggest a structure of the coupling site as shown in Figure 3C.

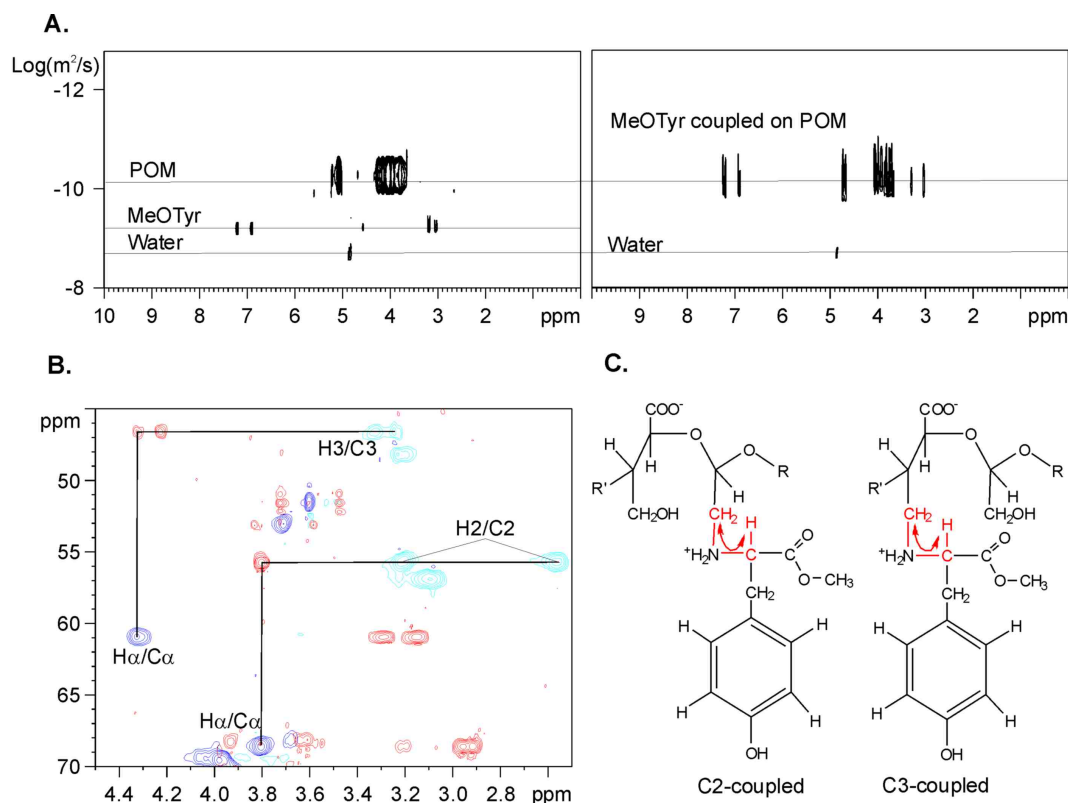


Figure 3: **A:** DOSY-spectra of a mixture of non-coupled POM and MeOTyr (left) and the coupled product POM-MeOTyr (right) in 99.9 % D₂O recorded at 25°C. **B:** Overlay of part of a ¹³C HSQC spectrum (blue:CH/CH₃; Cyan:CH₂) and a ¹³C HMBC spectrum (red) recorded for POM-MeOTyr in 99.9 % D₂O at 25°C. The lines show a three bond correlation from the H_α/C_α- to the H₂/C₂- or H₃/C₃ peak. Two additional signals for methylene-groups (-CH₂) are observed indicating formation of two new primary alcohol groups. **C:** Molecular structure of POM-MeOTyr based on the obtained NMR results. The part highlighted in red with an arrow shows the three bond correlation from HMBC, which confirm the coupling between mannuronan and MeOTyr.

Coupling to alginates with different chemical compositions

Five alginates with varying G content ranging from 0 - 85 % (Table 1) were oxidized (D_{ox} = 8 %) and subsequently coupled to MeOTyr using the optimized protocol (Figure 4A). Mannuronan (0 % G) gave the highest DS varying around the theoretical DS (8 %). Using a bacterial alginate with only 6 % G lowered the DS substantially (DS slightly below 5 %) and further increasing the G content resulted in increasing DS values. However, an in vitro epimerized alginate with 85 % G could not reach the same DS as mannuronan.

The observed differences in DS for different alginates were analyzed by looking at the variation associated with the coupling method. For both mannuronan and the stipe alginate, three different batches of periodate oxidized material was substituted with MeOTyr in two-four parallel reactions each (in total 9 coupling reactions per alginate). An unpaired student T-test was performed using the pooled standard deviation of all reactions as the standard deviation and showed that the coupling efficiency is significantly different ($p < 0.05$) using oxidized mannuronan ($DS_{\text{average}} = 8.6 \pm 0.3 \%$) relative to oxidized stipe alginate ($DS_{\text{average}} = 6.1 \pm 0.2 \%$) as starting materials (Figure 4B).

Aromatic molecules like MeOTyr also enable quantification of DS by both UV spectroscopy and fluorescence spectroscopy, serving as independent and experimentally simpler approaches compared to NMR. The same samples were therefore analyzed by UV spectroscopy for further verification of the observed differences. The DS obtained from UV spectroscopy was slightly lower than those obtained by $^1\text{H-NMR}$ spectroscopy with a DS of $6.4 \pm 0.2 \%$ for mannuronan and $5.2 \pm 0.2 \%$ for the stipe alginate (Figure 4B). However, the same tendencies were observed, namely that using mannuronan as the starting material gave a significant higher DS ($p < 0.05$) than what was possible to obtain using stipe alginate.

Some of the samples of both stipe POA-MeOTyr and POM-MeOTyr were also analyzed by fluorescence spectroscopy. The emission was measured in the range 280 nm to 380 nm, using 274 nm as the excitation wavelength (Figure S1 in supplementary data), but the emitted fluorescence from the tyrosine-ester was overshadowed by rayleigh scattering from water. In addition the data suggested that the emission intensity of MeOTyr coupled to POA or POM was quenched as it had values in the same range as the background emission.

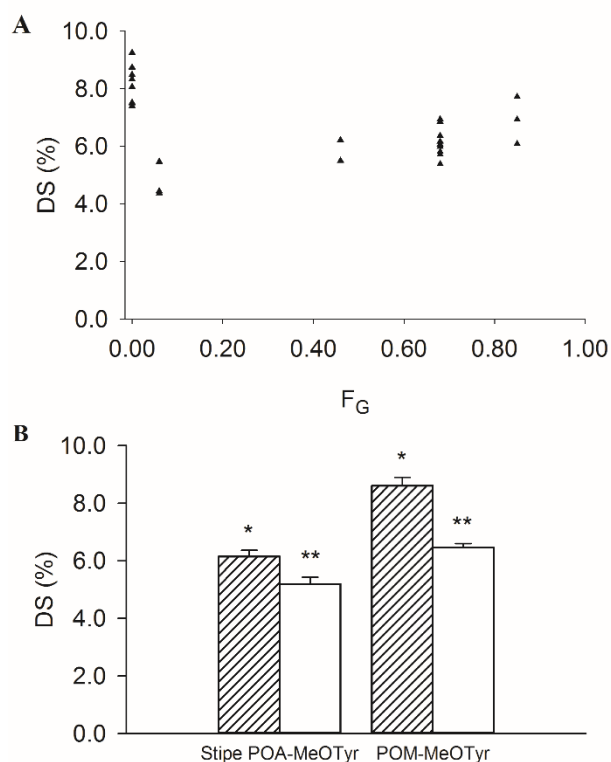


Figure 4: A: DS (%) as a function of fraction of G residues (F_G) in the alginate. Each dot represents a separate result using the optimized protocol and analyzed by $^1\text{H-NMR}$ ($F_G = 0.00$: $n = 9$, $F_G = 0.06$: $n = 3$, $F_G = 0.46$: $n = 2$, $F_G = 0.68$: $n = 9$, $F_G = 0.85$: $n = 3$) B: Three batches of stipe POA ($D_{\text{ox}} = 8\%$) and three batches of POM ($D_{\text{ox}} = 8\%$) were substituted with MeOTyr using the optimized protocol. Two-four parallel reductive amination reactions were performed for each batch and DS was determined using both $^1\text{H-NMR}$ (shaded bars) and UV spectroscopy (open bars). DS are given as the mean and error bars are given as the pooled standard deviation of different batches of the same material. Symbols * and ** designates internally significant differences ($p < 0.05$).

Coupling of short peptide sequences

Three different peptides, GRGDYP, KHIFSDDSSE and GRGDSP were coupled to leaf POA using the optimized protocol. Both GRGDYP and KHIFSDDSSE have aromatic residues, and DS can therefore be estimated as for MeOTyr. DS for leaf POA-GRGDSP was calculated according to the annotation by Sandvig et al [20]. Similarly to the model molecule we were able to obtain a high DS (3.9 – 6.9 %) for all three peptides (see Table 2). GRGDYP was also coupled to stipe POA ($D_{\text{ox}} = 8\%$) giving a slightly higher DS (4.7 %) compared to the reaction with the oxidized leaf alginate (DS = 3.9 %). Their respective $^1\text{H-NMR}$ spectra are shown in supplementary data (fig S2- S5).

Table 2: DS (%) determined from ¹H-NMR spectroscopy for different peptide sequences coupled to *L. hyperborea* leaf- and stipe POA (D_{ox} = 8 %).

Peptide	Alginate	DS (%)
KHIFSDDSSE	Leaf POA	6.9 %
GRGDSP	Leaf POA	4.1 %
GRGDYP	Leaf POA	3.9 %
GRGDYP	Stipe POA	4.7 %

Myoblast/dental stem cells attachment to peptide alginate hydrogels

Calcium alginate gels were made of leaf POA-GRGDSP (Table 2) in combination with non-coupled stipe alginate to obtain different concentrations of peptide while retaining gel strength. Cells were seeded on top of the gels, using the same seeding densities in all cases. The dental stem cells (RP89) and myoblasts (C2C12) are adhering cells and demonstrate a fibroblast-like and spindle shaped appearance in regular culture (Figure 5A). When no leaf POA-GRGDSP was present in the gels, no adhering cells were observed (Figure 5B). Both cell types became round shaped and formed cell clusters that were easily washed off the gel. When the stipe alginate was mixed with leaf POA-GRGDSP, the C2C12 cells adhered to the gels for all tested concentrations of GRGDSP (Figure 5, left panel C1-C4). The cells were well spread on the surface of the gels and presented with similar morphology for all concentrations of GRGDSP peptide, except for the lowest concentration of 0.1 % mol peptide per mol uronic acid where the cells still adhered to the surface but appeared in larger clusters that were connected with extensions (Figure 5, left panel C1). For the RP89 cells, cells adhering to the alginate gels were only observed with the highest concentration of GRGDSP, i.e. 1 % mol per mol uronic acid (Figure 5, right panel C4) and the cells presented as large cells that were stretched out in the longitudinal direction. A transition was seen at a lower peptide concentration with 0.5 % mol peptide per mol uronic acid where both clusters and some few adhering cells could be observed on the gel. Some degree of cell infiltration into the GRGDSP substituted alginate hydrogel was observed for both cell types as cells were observed in different focal planes (Figure 5, left panel C1-C4, right panel C3-C4) resulting in unclear images for parts of the pictures presented. As controls, RP89 and C2C12 cells were also cultured on alginate gels of stipe alginate combined with leaf POA where no peptide was present. No cells adhered to the gels regardless of the concentration of oxidized alginate (figure 5, D1-D4), demonstrating that the adherence of the cells was due to the presence of

the GRGDSP substituted leaf alginate. It should be noted that the apparent low cell numbers for the higher concentrations of peptides for RP89, as well as for the negative controls relative to positive controls and peptide-alginates, is attributed the selection of image area: clusters were found in more concentrated areas on the gel whereas the attached cells were more homogeneously distributed on the alginate gel surface.

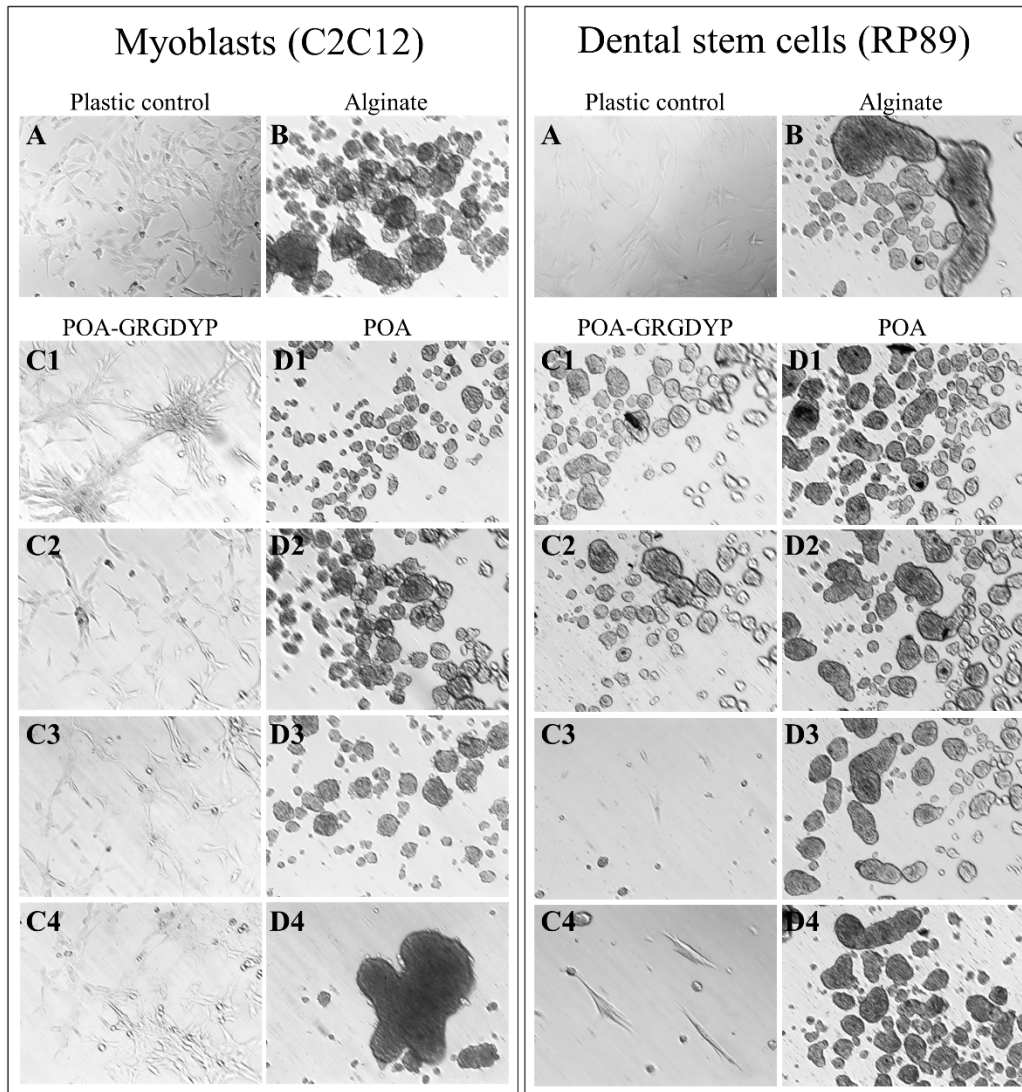


Figure 5: Culture of myoblasts (C2C12, left panel) and dental stem cells (RP89, right panel) on *L. hyperborea* alginate gels containing different concentrations of GRGDSP substituted leaf alginate 48 hours after seeding. **A:** Plastic control (normal culture conditions). **B:** Stipe alginate with no peptide. **C1-C4:** Cells on stipe alginate combined with different amounts of leaf POA-GRGDSP (DS = 4.1 %) to a total of 1% (w/v) alginate corresponding to finale peptide concentrations of: 0.1 % (C1), 0.25 % (C2), 0.5 % (C3) and 1 % (C4) mol peptide per mol uronic acids. **D1-D4:** Cells on stipe alginate combined with leaf POA to a total of 1% alginate (w/v) at concentrations corresponding to concentration of leaf POA-GRGDSP in C1-C4 respectively.

Discussion

Here, we show that high degrees of substitution and high coupling efficiencies with no detectable formation of by-products can be obtained on alginates by the covalent coupling of primary amines with reductive amination following periodate oxidation. The process was optimized using the non-toxic pic-BH₃ as the reducing agent. The biological activity of peptide-substituted materials was demonstrated in a cell attachment study also demonstrating the need for high peptide concentrations for dental stem cells to adhere.

Method development and characterization

In the optimization of reaction parameters, all the coupling reactions were successful with high DS in the range 2-6 % (Figure 2C-F). Pic-BH₃ can hence replace NaCNBH₃ as the reducing agent, which eliminates the safety precautions associated with NaCNBH₃ and the reaction product cyanide gas. The concentration of pic-BH₃ showed to have the most protuberant effect on DS, and peptide consumption could here be minimized using a higher concentration of pic-BH₃. Most of the literature on reductive amination is, to our knowledge, related mainly to general organic synthesis [30], or labelling of the reducing ends for quantitative mass spectroscopy [31, 32]. Grafting of peptides to a “poly aldehyde guluronate” by reductive amination using NaBH₃CN has been reported [41]. However, no focus on optimization of procedure and characterization of the product was shown.

The method enables tailoring of several aspects of alginates' material properties. Varying the initial D_{ox} will enable tuning of the final DS as well as the gel forming properties [40]. It is previously shown that one may assume stoichiometry for oxidation up to at least D_{ox} = 8 % and that only one aldehyde per oxidized residue would react with the substituent [42]. The theoretical DS using this strategy will hence be approximately equal to D_{ox} with an additional contribution from substitution at the reducing end of the polymer. Reaction time of the reductive amination can further be used to regulate the fraction of free oxidized residues (not participating in coupling). This may affect properties such as chain extension and rate of degradation of the modified alginate [43]. In addition pH offers to some extent a means to adjust the balance between substitution and degradation during the coupling reaction: Limited degradation occurred at pH 4.5 while maximum DS was obtained at pH 5.8. Increasing pH resulted in increased degradation (Figure 2G and H) which is attributed to alkaline β-elimination of the oxidized residues [43].

In general, the DS values reported here is higher than what has been obtained with carbodiimide chemistry [14, 19, 20] which enables studies of the effect of peptide densities in a wider range. Another aspect in comparing reductive amination with carbodiimide chemistry is the formation of by-products associated with the latter that cannot be removed by dialysis and coal filtration [20]. By-

products could not be identified in the ^1H -NMR spectra after reductive amination and subsequent analysis by DOSY (Figure 3A) showed that excess substituent could be removed by dialysis.

Verification of covalent coupling between POM and MeOTyr

Covalent coupling between POM and MeOTyr was verified using two different NMR approaches. DOSY are often used in NMR spectroscopy to separate the signals from different molecules in complex mixtures based on their diffusion coefficients [44]. Here, the DOSY spectra in Figure 3A show that POM and MeOTyr has different diffusion coefficients in the uncoupled sample while in the coupled sample MeOTyr diffused with the same rate as POM, indicating that covalent coupling is obtained. Although the method is an indirect proof of the coupling it can be very useful for evaluating coupling products with highly overlapping signals in the NMR spectrum. A DOSY measurement is also a less time demanding and user friendly NMR method compared to other indirect NMR methods like relaxation measurements.

In the second approach the HMBC spectrum gives a direct proof of the coupling as one can directly follow the correlations through the chemical bonds and verify that the molecules are covalently bound (Figure 3B). However, extracting information from the HMBC spectrum is reliant on well separated and assigned signals from other NMR spectra (e.g. HSQC). In the HSQC spectrum some additional signals were observed that indicate the presence of additional methylene groups. This may be due to the formation of primary alcohol groups, as a result of a reduction of the non-coupled aldehyde groups on C2 and/or C3 during the coupling reaction.

Reaction kinetics

A controllable DS and high coupling efficiency is preferred. However, high DS, using the preferable low concentrations of peptide, could only be achieved using high concentrations of the reducing agent (pic-BH₃). The Schiff base formation (Figure 1) is generally accepted to be the rate limiting step in reductive aminations, which further would imply that increasing the concentration of the reducing agent should not have a considerable effect on the net reaction rate. Sun et al [45] has presented a kinetic model showing that increasing the concentration of reducing agent will increase the amount of reaction product provided that the rate of Schiff base decomposition is negligible. We could model our data (not shown) as simple second order reactions where the effect of changing the amount of reducing agent on DS could be explained, similarly to Sun et al [45], by a decreasing difference in the rates of Schiff base formation and Schiff base reduction.

Another observation was that DS reached a plateau below the theoretical values (Figure 2 C-F). A prerequisite for complete quantitative reductive amination is to use reducing agents where the reduction of carbonyls is negligible (very slow) compared to the reduction of Schiff bases. Carbonyl

reduction has been observed for both pic-BH_3 and NaCNBH_3 [31, 46]. If pic-BH_3 reduces aldehydes and ketones at a substantial rate the available dialdehydes would be reduced during the reaction. Hence, it will not be possible to reach the theoretical DS. The same effect was theoretically predicted by Sun et al [45] and was also seen by altering the rate of carbonyl reduction in our reaction model. This is also supported by the observation of signals in the HSQC spectrum indicating reduction of the non-coupled aldehyde groups in the final reaction product.

The highest DS was obtained using pH 5.8, whereas increasing the pH to 7.5 or decreasing to pH 4.5 gave lower DS (48 h) (Figure 2E). Schiff base formation is dependent on protonation of the carbonyl oxygen and in addition the amino group has to be on its deprotonated form. For substituents (amines) with high pK_a values the optimal pH will therefore be a compromise between these two factors [45]. The α -amino group of amino acids has a pK_a around 6.8-8.0 and the results indicated that pH 7.5 was not acidic enough for pronounced protonation of the carbonyl oxygen, while pH 4.5 was too acidic for the amino group on MeOTyr to be highly deprotonated. DS increased depending on the substituent in the order $\text{KHIFSDDSSSE} > \text{MeOTyr} > \text{GRGDYP} \approx \text{GRGDSP}$. These differences might be the effect of the pK_a and hence, the equilibrium between the protonated and deprotonated form, of their respective N-terminal amino group at a certain pH. This will be influenced by both the nature of the N-terminal amino acid as well as the following residues in the peptide. GRGDYP and GRGDSP have the first four amino acids in common and the obtained DS differed within the variation associated with the coupling method (0.2 - 0.3 %).

Coupling to alginates with different chemical composition

Two main observations were done when MeOTyr was coupled to alginates with different chemical compositions: Coupling to mannuronan (0 % G) was the only reaction that gave theoretical DS (= D_{ox}) and alginates with increasing G content (6 % G - 85 % G) showed a trend for increasing DS (Figure 4A). Statistical analysis showed that the obtained DS for POM-MeOTyr (0 % G) and stipe POA-MeOTyr (65 % G) can be considered significantly different ($p < 0.05$). Higher DS was also observed in coupling of GRGDYP to stipe POA (65 % G) than to leaf POA (46 % G) (Table 2). The variation in DS will here reflect the variation associated with the method as a whole, including variation in D_{ox} between different periodate oxidized alginate batches, variation in DS for coupled samples from the same batch of periodate oxidized alginate and variation in the analysis of DS. The reason for the observed differences using different alginates was not further investigated and can therefore only be speculated to be due to differences in the conformation of the polymer or that the reaction kinetics is different for M and G. An important aspect is that the periodate oxidation is faster (50 %) on G than on M [47] and in an alginate containing G the reactive residues in the coupling reaction will hence be mainly G.

Determining DS: Comparison of UV- and NMR spectroscopy

To compare DS obtained from NMR- and UV spectroscopy several parallel reactions each of stipe POA-MeOTyr and POM-MeOTyr was analyzed by both methods. In general, UV-spectroscopy gave somewhat lower DS values than NMR spectroscopy (Figure 4B), however, both methods showed higher DS for stipe POA-MeOTyr than for POM-MeOTyr. The DS is here calculated as the percentage of alginate residues substituted with the target molecule and the calculation from absorbance data is therefore dependent on knowing the exact amount of alginate in the samples, which further will be dependent on the water content of the alginate. It has earlier been estimated that the water content in alginate after drying is approximately 10 % [48], but it may vary depending on e.g. alginate type and humidity and will hence influence the concentrations. In contrast, calculations from NMR data are based on signal intensities that are directly proportional to the number of protons giving rise to the signal. At low DS the accuracy will be influenced by the signal to noise ratio in the spectra.

Myoblast and dental stem cell attachment to alginate-GRGDSP gels

GRGDSP, GRGDYP and the neuropeptide KHIFSDDSSSE were all successfully coupled to both leaf and stipe POA. All three peptides are relevant for tissue engineering due to their bioactive properties. The RGD sequence has previously been demonstrated to be active on both myoblasts [14, 15, 20] and dental stem cells [49-51] and the GRGDSP coupled alginate was therefore used in the attachment studies to study both cell types in the same peptide-alginate system.

In studies of myoblast attachment to alginate hydrogel surfaces with covalently attached RGD-peptides by Rowley and Mooney [14] and later by other groups including ours [19, 20] the RGD-peptide has been covalently linked to the carboxylic group of the alginate resulting in about 0.1 – 1.0 % of monomers having a peptide substituent. In the present study, using the coupling strategy of periodate oxidation and subsequently reductive amination, 3.9 – 4.7 % of the monomers were substituted with RGD-peptide (Table 2). Leaf POA-GRGDSP (DS = 4.1 %) was mixed with alginate not containing peptide to retain gelling properties, resulting in gels with final concentrations of peptide varying from 0.1 % to 1 % (mol peptide/mol uronic acid monomers). The myoblasts seemed unaffected by the increase in peptide concentrations, however showed cluster formations at the lowest peptide concentration, still attached to the hydrogel surface, with interconnective extensions. In the early work by Rowley and Mooney [14] C2C12 myoblast attachment to RGD-alginate was shown to depend on the peptide concentration as well as the composition of the alginate. Our observations for the lower peptide concentrations match in observations with cluster formation of the myoblasts. For the higher peptide concentrations we did not observe differentiation, as exhibited by myoblast fusion into multinucleated myofibrils [14], however this could be due to the shorter time of observation in our study, different cell concentrations as well as an expected reduction of the stiffness of the gel due

to the mix of an alginate with a high G content with an alginate with a lower G-content with disrupted G-blocks due to oxidation and subsequent substitution with peptide.

The RP89 cells did not adhere to the surfaces with low peptide content, however at 1 % mol peptide/mol uronic acid monomers and partly at 0.5 % mol peptide/mol uronic acid monomers, the cells adhered and long, large, elongated cells were observed (Figure 5, right panel C4). Although the cells adhered and changed morphology, the attachment of the cells was weak and the cells lost their morphology after staining for viability (results not shown). Indeed, dental stem cells have previously been shown to attach to fibronectin-coated surfaces [50] and also to YRGDS coated PEGDA hydrogels [49]. In the latter case large attached cells were observed, using high concentrations of YRGDS (2 mM vs 0.5 mM for 1 % mol peptide/mol uronic acid monomers in this study). Also, Thein-Han et al. [51] showed that calcium-phosphate cement coated with RGD peptide, fibronectin or a platelet concentrate increased the attachment and proliferation of dental stem cells. When dental stem cells were encapsulated in commercially available RGD-alginate made using carbodiimide chemistry, they mostly remained round and only developed very short cytoplasmic extensions [52, 53], albeit a positive effect of the RGD-peptide was seen on cell viability [52]. Similar observations have also been made on other cell types in 3D culture in RGD-modified alginates such as mesenchymal stem cells [13] and osteosarcoma cells [54]. Hence, in particular for the dental stem cells an interesting follow-up will be to increase the concentration of RGD-peptide further, investigate other relevant peptides for attachment (e.g. the neuropeptide), as well as investigating the 3D culture of cells in alginate gels with high peptide concentrations. Peptide concentrations can be increased in the current system by increasing the concentration of peptide-alginate in the mixture with gelling alginates. However, as the G-blocks and hence the ability to form crosslinks are partly disrupted in the peptide-alginate, reduced mechanical strength will be expected as previously shown for chemically modified alginates [40, 55]. It may therefore be advantageous to add a relatively small amount of a high-DS peptide alginate (< 20% by mass) to the unmodified alginate to maintain the mechanical properties of the alginate gel, as compared to substituting all alginate chains to obtain the same finale (average) DS. Another solution will be to use an alginate with a higher G-content for the coupling of peptide, as we have demonstrated higher degrees of coupling to alginates with increasing G-content (Figure 4). In addition these alginates initially have more G-blocks and thus a higher degree of crosslinking is expected. A possible strategy will also be to couple the peptide to mannuronan, resulting in a very pure product where about all oxidized sugar units are grafted, with subsequent introduction of the crosslinking G-blocks by epimerization [7, 8, 20]. This chemoenzymatic strategy [20, 40] will allow the formation of alginate hydrogels with tailored mechanical properties and with varying and high concentrations of bioactive molecules.

Conclusion

This study presents an efficient method for coupling of bioactive molecules to alginates through partial periodate oxidation followed by reductive amination, where pic-BH₃ was established as a nontoxic alternative to NaCNBH₃, with similar efficiencies. We were able to obtain high DS confirmed by both NMR and UV spectroscopy, and covalently bound substituents were further confirmed by NMR. DS can be tuned changing the D_{ox} of the starting material or the reaction parameters. Due to the high grafting densities, altered polymer properties and the absence of covalent bound by-products, the method is considered a good alternative to the traditional carbodiimide chemistry. The importance of increased functionalization was further demonstrated by seeding of C2C12 myoblasts and RP89 dental stem cells onto alginate-peptide gels. In contrast to C2C12 myoblasts, the RP89 cells only adhered to the alginate gels with the highest concentrations of peptide. The DS was dependent on the composition of the alginate starting material and was highest for periodate oxidized mannuronan. A chemoenzymatic approach can then be used to first obtain a fully substituted alginate (DS = D_{ox}) and then enzymatically introduce G residue to acquire the gelling properties.

Acknowledgements

This work was supported by NTNU (project 81726300) and the Norwegian Research Council (grants 221576 (Marpol) and 227472). Dr. Ioanna Sandvig (Department of Neuroscience, NTNU) is acknowledged for the access to cell laboratories. We also thank Prof. Hallvard Fjøsne Svendsen (Department of Chemical Engineering, NTNU) for developing the kinetic model for reductive amination.

Appendix A. Figures with essential color discrimination

Certain figures in this article are difficult to interpret in black and white. The full color images can be found in the on-line version on ScienceDirect.

Appendix B. Supplementary data

Supplementary data related to this article can be found at (link to be inserted)

References

- [1] N.C. Hunt, L.M. Grover, Cell encapsulation using biopolymer gels for regenerative medicine, *Biotechnol. Lett.* 32 (2010) 733-742.
- [2] T. Dvir, B.P. Timko, D.S. Kohane, R. Langer, Nanotechnological strategies for engineering complex tissues, *Nat. Nanotechnol.* 6 (2011) 13-22.
- [3] T. Andersen, B.L. Strand, K. Formo, E. Alsberg, B.E. Christensen, Alginates as biomaterials in tissue engineering, in: A.P. Rauter, T. Lindhorst, (Eds), *Carbohydrate Chemistry: Chemical and Biological Approaches*, Royal Society of Chemistry, Cambridge, 2012, pp. 227-258.
- [4] K.Y. Lee, D.J. Mooney, Alginate: Properties and biomedical applications, *Progr. Polym. Sci.* 37 (2012) 106-126.
- [5] A.M. Rokstad, O.L. Brekke, B. Steinkjer, L. Ryan, G. Kollarikova, B.L. Strand, G. Skjåk-Bræk, I. Lacik, T. Espevik, T.E. Mollnes, Alginate microbeads are complement compatible, in contrast to polycation containing microcapsules, as revealed in a human whole blood model, *Acta Biomater.* 7 (2011) 2566-2578.
- [6] I. Donati, Y.A. Mørch, B.L. Strand, G. Skjåk-Bræk, S. Paoletti, Effect of elongation of alternating sequences on swelling behavior and large deformation properties of natural alginate gels, *J. Phys. Chem. B* 113 (2009) 12916-12922.
- [7] Y.A. Mørch, S. Holtan, I. Donati, B.L. Strand, G. Skjåk-Bræk, Mechanical properties of C-5 epimerized alginates, *Biomacromolecules* 9 (2008) 2360-2368.
- [8] Y.A. Mørch, I. Donati, B.L. Strand, G. Skjåk-Bræk, Molecular engineering as an approach to design new functional properties of alginate, *Biomacromolecules* 8 (2007) 2809-2814.
- [9] O. Aarstad, B.L. Strand, L.M. Klepp-Andersen, G. Skjåk-Bræk, Analysis of G-block distributions and their impact on gel properties of in vitro epimerized mannuronan, *Biomacromolecules* 14 (2013) 3409-3416.
- [10] M. Gimmetstad, H. Sletta, H. Ertesvåg, K. Bakkevig, S. Jain, S. Suh, G. Skjåk-Bræk, T.E. Ellingsen, D.E. Ohman, S. Valla, The *Pseudomonas fluorescens* AlgG protein, but not its mannuronan C-5-epimerase activity, is needed for alginate polymer formation, *J. Bacteriol.* 185 (2003) 3515-3523.
- [11] E. Buchinger, D.H. Knudsen, M.A. Behrens, J.S. Pedersen, O.A. Aarstad, A. Tøndervik, S. Valla, G. Skjåk-Bræk, R. Wimmer, F.L. Aachmann, Structural and functional characterization of the R-modules in alginate C-5 epimerases AlgE4 and AlgE6 from *Azotobacter vinelandii*, *J. Biol. Chem.* 289 (2014) 31382-31396.
- [12] J. Stenvik, H. Sletta, O. Grimstad, B. Pukstad, L. Ryan, R. Aune, W. Strand, A. Tøndervik, S.H. Torp, G. Skjåk-Bræk, T. Espevik, Alginates induce differentiation and expression of CXCR7 and CXCL12/SDF-1 in human keratinocytes -the role of calcium, *J. Biomed. Mater. Res. A* 100 (2012) 2803-2812.
- [13] K.B. Fonseca, S.J. Bidarra, M.J. Oliveira, P.L. Granja, C.C. Barrias, Molecularly designed alginate hydrogels susceptible to local proteolysis as three-dimensional cellular microenvironments, *Acta Biomaterialia* 7 (2011) 1674-1682.
- [14] J.A. Rowley, D.J. Mooney, Alginate type and RGD density control myoblast phenotype, *J. Biomed. Mater. Res.* 60 (2002) 217-223.
- [15] J.A. Rowley, G. Madlambayan, D.J. Mooney, Alginate hydrogels as synthetic extracellular matrix materials, *Biomaterials* 20 (1999) 45-53.
- [16] E. Ruoslahti, RGD and other recognition sequences for integrins, *Ann. Rev. Cell Develop. Biol.* 12 (1996) 697-715.
- [17] O. Sporns, G.M. Edelman, K.L. Crossin, The neural cell-adhesion molecule (N-Cam) inhibits proliferation in primary cultures of rat astrocytes, *Proc. Nat. Acad. Sci.* 92 (1995) 542-546.
- [18] L. Kam, W. Shain, J.N. Turner, R. Bizios, Selective adhesion of astrocytes to surfaces modified with immobilized peptides, *Biomaterials* 23 (2002) 511-515.
- [19] K. Formo, C.H. Cho, L. Vallier, B.L. Strand, Culture of hESC-derived pancreatic progenitors in alginate-based scaffolds, *J. Biomed. Mater. Res. A* 103 (2015) 3717-3726.

- [20] I. Sandvig, K. Karstensen, A.M. Rokstad, F.L. Aachmann, K. Formo, A. Sandvig, G. Skjak-Braek, B.L. Strand, RGD-peptide modified alginate by a chemoenzymatic strategy for tissue engineering applications, *J. Biomed. Mater. Res. A* 103 (2015) 896-906.
- [21] S.J. Bidarra, C.C. Barrias, K.B. Fonseca, M.A. Barbosa, R.A. Soares, P.L. Granja, Injectable in situ crosslinkable RGD-modified alginate matrix for endothelial cells delivery, *Biomaterials* 32 (2011) 7897-7904.
- [22] N.O. Dhoot, C.A. Tobias, I. Fischer, M.A. Wheatley, Peptide-modified alginate surfaces as a growth permissive substrate for neurite outgrowth, *J. Biomed. Mater. Res. A* 71 (2004) 191-200.
- [23] T. Andersen, C. Markussen, M. Dornish, H. Heier-Baardson, J.E. Melvik, E. Alsberg, B.E. Christensen, In situ gelation for cell immobilization and culture in alginate foam scaffolds, *Tissue Eng. A* 20 (2014) 600-610.
- [24] G. Dryhurst, Periodate oxidation of diol and other functional groups; analytical and structural applications. Pergamon Press, Oxford, 1970.
- [25] A.S. Perlin, Glycol-cleavage oxidation, *Adv. Carbohyd. Chem. Bi.* 60 (2006) 183-250.
- [26] K.Y. Lee, K.H. Bouhadir, D.J. Mooney, Evaluation of chain stiffness of partially oxidized polyguluronate, *Biomacromolecules* 3 (2002) 1129-1134.
- [27] O. Smidsrød, T. Painter, Effect of periodate oxidation upon the stiffness of the alginate molecule in solution, *Carbohyd. Res.* 26 (1973) 125-132.
- [28] I.M.N. Vold, K.A. Kristiansen, B.E. Christensen, A study of the chain stiffness and extension of alginates, in vitro epimerized alginates, and periodate-oxidized alginates using size-exclusion chromatography combined with light scattering and viscosity detectors, *Biomacromolecules* 7 (2006) 2136-2146.
- [29] K.H. Bouhadir, K.Y. Lee, E. Alsberg, K.L. Damm, K.W. Anderson, D.J. Mooney, Degradation of partially oxidized alginate and its potential application for tissue engineering, *Biotechnol. Prog.* 17 (2001) 945-950.
- [30] S. Sato, T. Sakamoto, E. Miyazawa, Y. Kikugawa, One-pot reductive amination of aldehydes and ketones with alpha-picoline-borane in methanol, in water, and in neat conditions, *Tetrahedron* 60 (2004) 7899-7906.
- [31] L.R. Ruhaak, E. Steenvoorden, C.A.M. Koeleman, A.M. Deelder, M. Wuhrer, 2-Picoline-borane: A non-toxic reducing agent for oligosaccharide labeling by reductive amination, *Proteomics* 10 (2010) 2330-2336.
- [32] I. Unterrieser, P. Mischnick, Labeling of oligosaccharides for quantitative mass spectrometry, *Carbohyd. Res.* 346 (2011) 68-75.
- [33] J.A. Sirvio, A. Kolehmainen, M. Visanko, H. Liimatainen, J. Niinimäki, O.E.O. Hormi, Strong, self-standing oxygen barrier films from nanocelluloses modified with regioselective oxidative treatments, *ACS Appl. Mater. Interfaces* 6 (2014) 14384-14390.
- [34] G. Skjåk-Bræk, H. Grasdalen, B. Larsen, Monomer sequence and acetylation pattern in some bacterial alginates, *Carbohyd. Res.* 154 (1986) 239-250.
- [35] H. Ertesvåg, G. Skjåk-Bræk, Modification of alginate using mannuronan C-5-epimerases., in: C. Bucke, (Ed). *Methods in Biotechnology*, Humana press Inc, New Jersey, 1999, pp. 71-78.
- [36] Y.L. Xia, G. Legge, K.Y. Jun, Y.L. Qi, H. Lee, X.L. Gao, IP-COSY, a totally in-phase and sensitive COSY experiment, *Magn. Reson. Chem.* 43 (2005) 372-379.
- [37] N.B. Ruparel, J.F.A. de Almeida, M.A. Henry, A. Diogenes, Characterization of a stem cell of apical papilla cell line: Effect of passage on cellular phenotype, *J. Endodont.* 39 (2013) 357-363.
- [38] H. Grasdalen, B. Larsen, O. Smidsrød, Pmr study of the composition and sequence of uronate residues in alginates, *Carbohyd. Res.* 68 (1979) 23-31.
- [39] H. Grasdalen, High-field, H-1-NMR spectroscopy of alginate - sequential structure and linkage conformations, *Carbohyd. Res.* 118 (1983) 255-260.
- [40] K.A. Kristiansen, B.C. Schirmer, F.L. Aachmann, G. Skjåk-Bræk, K.I. Draget, B.E. Christensen, Novel alginates prepared by independent control of chain stiffness and distribution of G-residues: Structure and gelling properties, *Carbohyd. Polym.* 77 (2009) 725-735.

- [41] K.H. Bouhadir, D.S. Hausman, D.J. Mooney, Synthesis of cross-linked poly(aldehyde guluronate) hydrogels, *Polymer* 40 (1999) 3575-3584.
- [42] K.A. Kristiansen, S. Ballance, A. Potthast, B.E. Christensen, An evaluation of tritium and fluorescence labelling combined with multi-detector SEC for the detection of carbonyl groups in polysaccharides, *Carbohydr. Polym.* 76 (2009) 196-205.
- [43] K.A. Kristiansen, H.B. Tomren, B.E. Christensen, Periodate oxidized alginates: Depolymerization kinetics, *Carbohydr. Polym.* 86 (2011) 1595-1601.
- [44] C.S. Johnson, Diffusion ordered nuclear magnetic resonance spectroscopy: principles and applications, *Progr. Nucl. Mag. Res. Sp.* 34 (1999) 203-256.
- [45] Z.C. Sun, Z. Wei, K.M. Wei, A model for predicting the optimal conditions for labeling the carbohydrates with the amine derivatives by reductive amination, *Lett. Org. Chem.* 6 (2009) 549-551.
- [46] V.A. Cosenza, D.A. Navarro, C.A. Stortz, Usage of α -picoline borane for the reductive amination of carbohydrates, *Arkivoc* (2011) 182-194.
- [47] T. Painter, B. Larsen, Formation of hemiacetals between neighbouring hexuronic acid residues during periodate oxidation of alginate, *Acta Chem. Scand.* 24 (1970) 813-833.
- [48] A. Haug. Composition and properties of alginates. Trondheim, Norway, Norwegian Institute of Technology, 1964.
- [49] S.J. Dangaria, Y. Ito, C. Walker, R. Druzinsky, X.H. Luan, T.G.H. Diekwisch, Extracellular matrix-mediated differentiation of periodontal progenitor cells, *Differentiation* 78 (2009) 79-90.
- [50] J.S. Lee, H.S. Kim, S.Y. Park, T.W. Kim, J.S. Jung, J.B. Lee, C.S. Kim, Synergistic Effects of a Calcium Phosphate/Fibronectin Coating on the Adhesion of Periodontal Ligament Stem Cells Onto Decellularized Dental Root Surfaces, *Cell Transplant.* 24 (2015) 1767-1779.
- [51] W. Thein-Han, J. Liu, H.H. Xu, Calcium phosphate cement with biofunctional agents and stem cell seeding for dental and craniofacial bone repair, *Dent. Mater.* 28 (2012) 1059-1070.
- [52] A. Moshaverinia, C. Chen, X. Xu, K. Akiyama, S. Ansari, H.H. Zadeh, S. Shi, Bone regeneration potential of stem cells derived from periodontal ligament or gingival tissue sources encapsulated in RGD-modified alginate scaffold, *Tissue Eng. A* 20 (2014) 611-621.
- [53] A. Moshaverinia, X. Xu, C. Chen, S. Ansari, H.H. Zadeh, M.L. Snead, S. Shi, Application of stem cells derived from the periodontal ligament or gingival tissue sources for tendon tissue regeneration, *Biomaterials* 35 (2014) 2642-2650.
- [54] A. Grigore, B. Sarker, B. Fabry, A.R. Boccaccini, R. Detsch, Behavior of Encapsulated MG-63 Cells in RGD and Gelatine-Modified Alginate Hydrogels, *Tissue Eng. A* 20 (2014) 2140-2150.
- [55] I. Donati, K.I. Draget, M. Borgogna, S. Paoletti, G. Skjåk-Bræk, Tailor-made alginate bearing galactose moieties on mannuronic residues: Selective modification achieved by a chemoenzymatic strategy, *Biomacromolecules* 6 (2005) 88-98.